Excitation Energy-Dependent, Excited State
Intramolecular Proton Transfer-Based Dual
Emission in Poor Hydrogen-Bonding Solvents

Joseph J. M. Hurley and Lei Zhu*

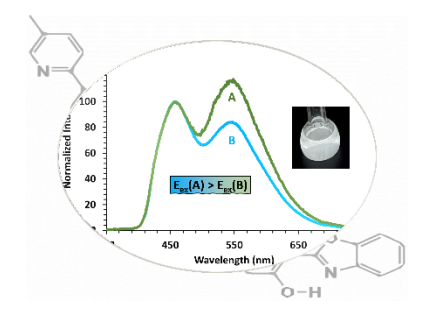
Department of Chemistry and Biochemistry, Florida State University, 95 Chieftan Way, Tallahassee, Florida 32306-4390, United States

Corresponding Author

* lzhu@fsu.edu

ABSTRACT. 2-(2'-Hydroxyphenyl)benzoxazole (HBO) substituted at the 5'-position with bipyridylvinylene phenylenevinylene (compound 2) produces both normal and, via an excited state intramolecular proton transfer (ESIPT) reaction, tautomer emissions in solvents that preserve intramolecular hydrogen bonds. The abundance of the tautomer emission from compound 2 in a poor hydrogen-bonding solvent increases in response to the application of a higher excitation energy. Based on quantum chemical calculations, the excitation-dependent dual emission is consistent with a model where the ESIPT reaction is more favored in the S₂ than in the S₁ electronically excited state.

TOC GRAPHICS



KEYWORDS. Excitation-dependence; dual emission; excited state intramolecular proton transfer (ESIPT), 2-(2'-hydroxyphenyl)benzoxazole (HBO)

Introduction

The need for organic emitters in light-emitting devices is one impetus that drives the discovery of dyes capable of dual emission.¹ One effective strategy is to incorporate the capability of excited state intramolecular proton transfer (ESIPT)²⁻⁴ in a dye. A lead compound for this purpose is 2-(2'-hydroxyphenyl)benzoxazole (HBO, Scheme 1),^{5,6} which in a poor hydrogenbonding solvent emits primarily from the excited state proton-transferred tautomer (aka the keto form, K in Scheme 1). In a hydrogen-bonding solvent, the solvation process becomes considerable (Scheme 1), which leads to the formation of the solvated enol (SE) in the ground state that affords its normal (aka the enol) emission. Upon thoughtful selection of solvent and/or the introduction of additives (e.g., a base, which could trigger the formation of the anion in Scheme 1^{6,7}), some HBO derivatives⁸⁻¹⁰ and other fluorophores¹¹ may afford white emission - a sought-after consequence that raises prospects of practical uses.¹²

Scheme 1. The ground and excited state processes that produce emitters of a HBO derivative.^a

a. B = base, S = hydrogen bond-accepting solvent. The acronym of each species is written in red: E = enol; K = keto; A = anion; SE = solvated enol. The depicted compound is HBO when R = H. Within the blue boundaries are the species projected to exist in a non-hydrogen-bonding solvent without any additive (e.g., a base).

Rarer are bright fluorophores that emit in a given composite color, including white, in the absence of a strong solvent interaction. ¹³⁻¹⁶ The practical value of such an emitter would increase if the color could be changed via excitation energy. On the fundamental front, creating dyes capable of excitation-dependent dual emission without assistance from the solvent or an additive represents a formidable challenge, as most photochemistry is known to occur on the first electronically excited state and therefore is predestined for an outcome independent of excitation energy. ¹⁷⁻¹⁹ In this work, we present a case in which an HBO derivative emits excitation-dependent dual emission in the absence of strong solvation, and we offer an explanation on the excitation energy-dependent emission property that is supported by quantum chemical calculations.

Methods

Experimental. Reagents and solvents were purchased from various commercial sources and used without further purification unless otherwise stated. Spectroscopic grade solvents were used in the UV/VIS and fluorescence spectroscopic measurements. Samples of spectroscopy were prepared in borosilicate volumetric flasks and transferred to quartz cuvettes using Hamilton gastight borosilicate syringes. The uses of lime glass Pasteur pipets and latex rubber bulbs were avoided in sample preparations due to the increased likelihood of accidental deprotonation of the dye.⁶ All reactions were carried out in oven- or flame-dried glassware in an inert atmosphere of argon. Analytical thin-layer chromatography (TLC) was performed using pre-coated TLC plates with silica gel 60 F254. Flash column chromatography was performed using silica (230-400 mesh) gel as the stationary phase. ¹H and ¹³C NMR spectra were acquired on Bruker AVANCE III NMR

Spectrometers with frequencies indicated in the synthetic procedures. All chemical shifts were reported in δ units relative to tetramethylsilane. CDCl₃ was treated with basic alumina gel prior to use. High resolution mass spectra were obtained at the Mass Spectrometry Laboratory at FSU. Steady state spectrophotometric and fluorometric measurements were conducted on a Varian Cary 100 Bio UV-Visible Spectrophotometer and a Varian Cary Eclipse Fluorescence Spectrophotometer, respectively. The synthetic procedures and additional spectroscopic data are listed in the Supporting Information.

Computational. All calculations were carried out using the quantum chemistry package TURBOMOLE V7.4.²⁰ The ground state geometries were optimized at the density functional level of theory (DFT) using the B3LYP functional²¹ and the def2-TZVP basis sets.²² The second derivatives were calculated using the 'aoforce' module to confirm the nature of the stationary points to be either minima (all real frequencies) or transition states (one imaginary frequency). The excited state geometric and electronic structural parameters were determined using the time-dependent DFT (TDDFT)²³ with the same functional and basis sets as listed above. The second derivatives of the minimized geometries of the excited states were calculated using the 'NumForce' module to distinguish between minima and transition states. The frontier molecular orbitals were plotted in Figure 5 using gOpenMol.^{24,25} Additional data of computation are listed in the Supporting Information.

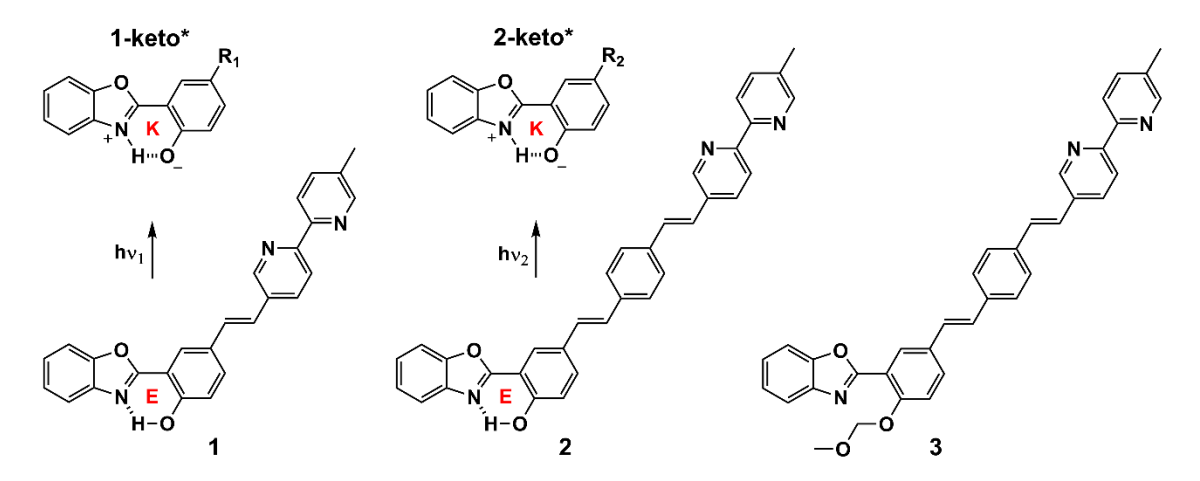
Results and Discussion

The previously reported compound $\mathbf{1}$ (Chart 1)⁸ exhibits excitation-dependent dual emission only in a hydrogen-bonding solvent such as N,N-dimethylformamide (DMF) or dimethyl sulfoxide (DMSO). The engagement of the HBO component in hydrogen bonding with the

solvent produces the solvated species (SE in Scheme 1). The SE and the intramolecularly hydrogen bonded population (E in Scheme 1) can be separately excited, which leads to the observed excitation dependence of the dual emission of 1.8 This is a case where solvent assistance is crucial in achieving the excitation-dependence of the dual emission. In a solvent such as dichloromethane (DCM) that is unlikely to form hydrogen bonds (HBs) with compound 1, predominantly the intramolecularly hydrogen-bonded species exist (depicted within the blue boundaries in Scheme 1), which ultimately affords the keto (K in Scheme 1) emission (Figure 1a, blue line) by way of ESIPT with little excitation dependence.

The inability of compound 1 to produce dual emission in a non-hydrogen bonding solvent prompted us to hunt for the structural factors that could result in both enol and keto emissions, the ratio of which would depend on excitation energy, from solely the intramolecularly hydrogen bonded form of a related compound. The solution offered in this work is compound 2 (Chart 1, center), which has a phenylenevinylene moiety between the vinylbipy and the HBO components found in compound 1. The synthesis of compound 2 is described in the Supporting Information. This compound was found stable against E/Z photoisomerization under ambient light based on the ¹H NMR and UV/vis spectroscopic evidence (Figures S1-4).

Chart 1. Structures of intramolecularly hydrogen-bonded compounds 1, 2, and the O-alkylated 3.^a



a. The enol and keto forms are marked as "E" and "K", respectively. The substituents at the 5'-positions of 1 and 2 are represented by 'R₁' and 'R₂' in their respective keto structures.

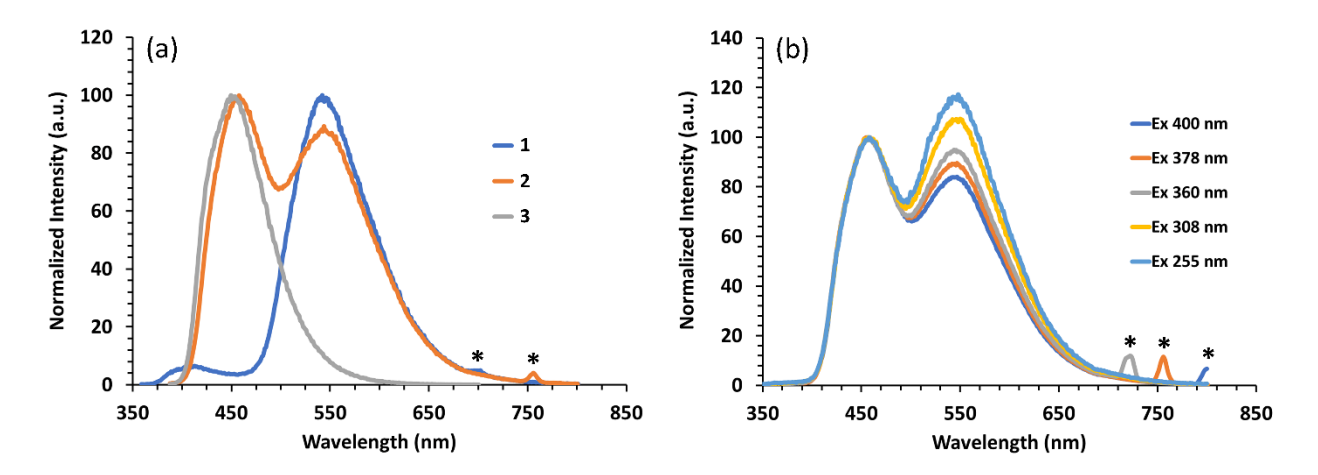


Figure 1. Normalized emission spectra of (a) compounds **1** (blue, 15 μ M, λ_{ex} = 349 nm. This spectrum was reproduced from Meisner, Q. J.; Younes, A. H.; Yuan, Z.; Sreenath, K.; Hurley, J. J. M.; Zhu, L. Excitation-Dependent Multiple Fluorescence of a Substituted 2-(2'-Hydroxyphenyl)benzoxazole. *J. Phys. Chem. A* **2018**, *122*, 9209-9223. Copyright 2018 American

Chemical Society), **2** (orange, 15 μ M, λ_{ex} = 378 nm) and **3** (gray, 15 μ M, λ_{ex} = 378 nm), and (b) compound **2** (5 μ M, λ_{ex} = 255-400 nm) in DCM. *: second order scatter bands.

The effect of solvent on the absorption and emission spectra of compound 2 are consistent with the expectations of an ESIPT-capable dye (Figure S5a,b) – that is to say, a more polar solvent prompts a higher abundance of the enol emission band from the solvated enol, while decreasing the polarity of the solvent leads to more of the keto emission with an abnormally large apparent Stokes shift.⁵ Two overlapping emission bands from 2 were observed in DCM (Figure 1a, orange line) – a solvent that would not engage in hydrogen bonding. The shorter wavelength band overlaps with the emission spectrum of compound 3 (Figure 1a, gray line), which is the O-alkylated analog with the intramolecular HB taken away. The longer wavelength band of 2 superimposes with the keto emission band of compound 1 (Figure 1a, blue line). These behaviors are consistent with the assignment of short- and long-wavelength bands of 2 to the emissions from its enol and keto excited states, respectively. Therefore, this is one of the rare cases 13,14,26 where the enol emission of an HBO derivative is found in a significant proportion in the overall emission in a poor hydrogen-bonding solvent, in which the intramolecularly hydrogen bonded progenitor of the keto form takes a predominant if not exclusive proportion in the ground state (Scheme 1 within the blue boundaries). The visual contrast between the emission colors of compounds 1 and 2 in DCM or toluene under UV irradiation is striking – compound 1 (Figure 2, top) shows a yellow emission color characteristic of that from the keto form, while an almost white color was observed from the sample of compound 2 (Figure 2, bottom), attributable to the balancing between its enol and keto emission bands that are spectrally resolved as shown in Figure 1 (orange line).

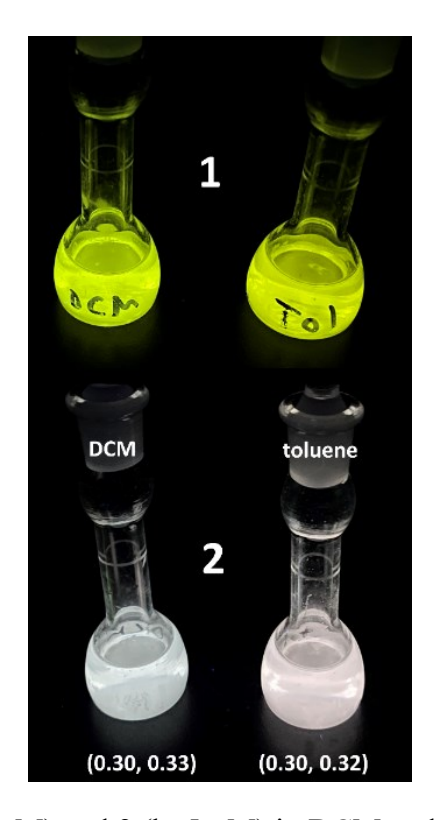


Figure 2. Compounds 1 (a, 15 μ M) and 2 (b, 5 μ M) in DCM and toluene under the irradiation of a handheld UV lamp ($\lambda_{ex} = 365$ nm). The CIE 1931 coordinates of the emissions from compound 2 are listed at the bottom.

When varying the excitation wavelength in DCM, the relative abundance of the enol and keto emissions of compound 2 appears to change - a longer excitation wavelength (i.e., lower excitation energy) favors the higher energy enol emission, while a shorter excitation wavelength (i.e., higher excitation energy) favors the lower energy keto emission (Figure 1b). The excitation spectra taken at enol and keto emission band maxima are shown in Figure S6. The excitation spectrum of the enol band has lower intensity on the high energy end than that of the keto band. The emission quantum yields (Table S1) and lifetime values (Tables S2-3) were also collected at various excitation wavelengths, and briefly analyzed in the Supporting Information.

Varying the excitation wavelength did not alter the band shape of the O-alkylated compound 3 (Figure S9), which suggests that (1) an intramolecular HB, and consequently, the ESIPT is a requirement for the excitation dependence of 2, and (2) the possible ground state conformational distribution, especially on the phenylenevinylene axis, is unlikely a contributor to the excitation dependence of 2 because the conformationally similar 3 does not exhibit any excitationdependent emission. The excitation dependence was also observed in toluene (Figure S10), which rules out that the excitation dependence is driven by the nature of the solvent (i.e., DCM). The possibility that two intramolecularly hydrogen bonded conformers of 2 might have been excited separately to result in excitation dependence was not supported by the analysis via quantum chemical calculations (Table S4). We did not find credible that ground state aggregation might have contributed to the excitation dependence because varying the concentration within 2-20 µM did not change either the absorption or the emission spectrum (Figures S11-12). The contamination of the sample of 2 with a miniscule amount of 3 was ruled out because in that case an excitation dependence in the opposite direction (i.e., a shorter excitation wavelength produces more enol emission) would have been observed (see the absorption overlays in Figure S13). The likelihood that acid, base, or metal ion contaminants may have led to the observed excitation dependence was not supported by evidence (Figures S14-17; brief analyses were also given in the Supporting Information).

The parent compound 1 in three non-hydrogen bonding solvents, hexanes, toluene, and DCM, exhibits little excitation dependence (Figure S18). The behavior of 1 is within the expectation based on the photophysical principle that the vast majority of photochemical reactions occurs on the S_1 (or T_1) state because the internal conversion (IC) from the higher electronic states to the S_1 (or T_1) is almost always faster than other processes. ¹⁷⁻¹⁹ In light of the skepticism of claims of

excitation-dependent emission from a small molecular dye,^{27,28} which is a rare event and should sustain rigorous control experiments and verification efforts, several batches of compound **2** were prepared independently, from which the excitation-dependent emission in DCM and toluene was reproduced. Based on this and the control experiments described earlier, the excitation-dependent dual emission of compound **2** in an intramolecular HB-preserving solvent is considered an innate property. This observation suggests that the ESIPT is favored at a higher excited electronic state than the first one, and in consequence, a shorter excitation wavelength results in a larger portion of the keto emission.

The molecular and electronic structures of compounds 1 and 2 in ground (S_0) and excited states (S₁ and S₂) were characterized computationally at the (TD)DFT/B3LYP/def2-TZVP level of theory. The S₁ and S₂ excitation energies and oscillator strengths at the optimized ground state geometries of 1 and 2 were calculated using the TDDFT/B3LYP/def2-TZVP and RICC2/def2-TZVP methods (Table S5). The B3LYP functional is widely used in (TD)DFT calculations of organic molecules under a relatively lean budget of computation.²⁹ The B3LYP is also a popular choice in (TD)DFT calculations of ESIPT-capable compounds. 4,30-33 However, the limitations of B3LYP have been extensively reported, which we have briefly summarized in a previous paper from our group. In particular, the excitation energy values of charge-transfer type molecules can be severely underestimated by the B3LYP functional. In the current study, we elected to continue to use B3LYP functional for several reasons: (1) there is a limited computational resource that is available to us which does not allow, for example, the application of the CC2 method for geometry optimizations of compounds 1 and 2 (50 and 64 atoms, respectively) within a reasonable time frame. (2) In the current work, there is a reference compound (1) to compare with the results from compound 2, which is the focus of the discussion. Therefore, the

differences in properties of these two compounds, rather than the absolute values of the computed data, are used to draw the conclusions. (3) There are precedents that utilize B3LYP in the calculations of S2 states (either geometry or excitation energy) of similarly sized molecular systems. 34-36 B3LYP has been reported to work in some cases even better than CAM-B3LYP, a functional that is considered more suitable for charge-transfer molecular systems. 35,37 Despite of these arguments that are specific to the current study, one, of course, shall always be mindful of the limitations of the B3LYP functional, which has been well documented, and, if possible, provide controls and other supporting evidence to back up the conclusion from the calculations.

The calculations revealed three distinctions between the two compounds that argue in favor of a faster ESIPT on the S₂ than the S₁ state for 2 but not 1, the first of which pertains to the energetics based on the calculated minimal energy reaction paths (MEPs)^{31,32,38-42} on both S₁ and S₂ states (Figure 3a,b) and the total energy values of the identified stationary points (minima and saddle points listed in Table 1). Having a +4.9 kcal/mol of the reaction energy (ΔE) and +7.8 kcal/mol of the barrier (ΔE^{\dagger}) on the OH coordinate of the S₁, compound 2 is less inclined to undergo the ESIPT on the S_1 surface both thermodynamically and kinetically than 1 ($\Delta E = -0.2$ kcal/mol, while $\Delta E^{\dagger} = 3.2$ kcal/mol using the same method, Table 1). The barrier of proton transfer of 2 on the S₂ (6.6 kcal/mol) is less than that on the S₁ (7.8 kcal/mol), while the opposite is true for 1.8 The difference in energy between the S₁ and the S₂ over the OH coordinate of 2 is plotted in the insets of Figure 3a, where a minimal gap is reached at an OH distance of ~ 1.2 Å. A minimum on the same S_2 - S_1 energy gap plot of 1 (Figure 3b inset) is absent. This comparison suggests that it is possible for the enol form of 2 on the S₂ state to slide to the S₁ (e.g., via a conical intersection) at ~ 1.2 Å OH distance, which then overcomes a small residual barrier to sink into the minimum of the S_1 keto form.

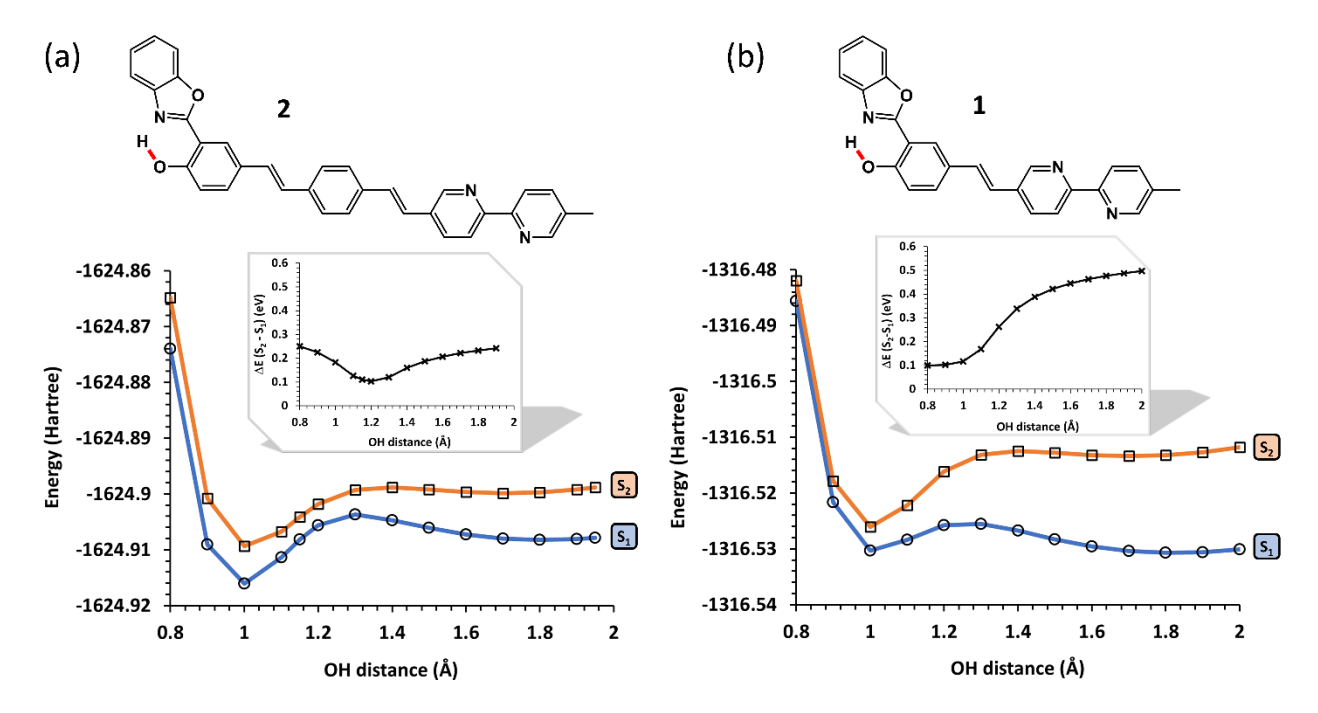


Figure 3. The minimal energy reaction paths (MEPs) of the S₁ (blue) and S₂ (orange) states of compounds **2** (a) and **1** (b) along the OH coordinates, calculated at the TDDFT/B3LYP/def2-TZVP level of theory. The structures of the compounds are shown above their MEPs. The OH bonds, the distances of which are the independent variables of the plots, are marked red in the structures. The energies are plotted to the same scale for the ease of visual comparison. The insets are the differences in energies between the S₂ and the S₁ over the OH coordinates. Both insets are plotted to the same scales on X and Y axes.

Table 1. Relative Total Energies (ΔE) and Geometries of Stationary Points on S₁ and S₂ States.^a

2	OH (Å)	NH (Å)	ΔE (kcal/mol)	1 ^b	OH (Å)	NH (Å)	ΔE (kcal/mol)
enol (S ₀)	0.99	1.78	A	enol (S ₀)	0.99	1.78	A'
$TS^{c}\left(S_{0}\right)$	1.47	1.10	A+11	$TS^{c}(S_{0})$	1.47	1.10	A'+11
keto (S ₀)	1.61	1.06	A+11	keto (S ₀)	1.62	1.06	A'+11
$enol\left(S_{1}\right)$	0.99	1.76	В	enol $(S_1)^d$	1.01	1.67	В'
$TS^{c}\left(S_{1}\right)$	1.27	1.23	B+7.8	$TS^{c}(S_{1})$	1.26	1.24	B'+3.2
keto (S_1)	1.81	1.03	B+4.9	keto (S ₁)	1.82	1.03	B'-0.2
enol $(S_2)^d$	1.01	1.68	C	enol (S ₂)	1.00	1.71	C'
$TS^{c}(S_{2})$	1.36	1.16	C+6.6	$TS^{c}(S_{2})$	1.40	1.14	C'+8.5
keto (S ₂)	1.71	1.04	C+6.0	keto (S ₂)	1.70	1.04	C'+8.0

a. The stationary points were identified on the MEPs and were optimized at the DFT or TDDFT/B3LYP/def2-TZVP level of theory without any constraints or consideration of solvent; b. The data of compound 1 was reproduced from Meisner, Q. J.; Younes, A. H.; Yuan, Z.; Sreenath, K.; Hurley, J. J. M.; Zhu, L. Excitation-Dependent Multiple Fluorescence of a Substituted 2-(2'-Hydroxyphenyl)benzoxazole. *J. Phys. Chem. A* 2018, *122*, 9209-9223. Copyright 2018 American Chemical Society; c. TS = transition state; d. shading emphasizes the elongation of the OH bond and the contraction of the NH hydrogen bond that precedes the ESIPT on either S₂ (for compound 2) or S₁ (for compound 1).

Next, the ratios of the NH distances of the S_1 and S_2 over that of the S_0 at each constrained OH length are plotted to reveal how the NH contracts or stretches on the S_1 and S_2 relative to the S_0 . The NH bond of **2** contracts more on the S_2 (orange in Figure 4a) at the enol geometry than on the S_1 (blue), suggesting a stronger tendency for the proton transfer from O to N on the S_2 than on the S_1 , while the opposite is true for compound **1** (Figure 4b; also see the shaded entries in Table 1). Meanwhile, the O-N distance is reduced in sync with the contraction of the NH distance of each compound (Figure S19), as to be expected in an ESIPT reaction. $^{43-48}$ At ~ 1.2 Å OH distance of **2**, the NH bonds of the S_2 and the S_1 coincide. The geometric convergence of the

S₂ and the S₁ states (in terms of the OH and NH distances) takes place at an OH distance where the energy gap between the S₂ and the S₁ reaches the minimum (inset of Figure 3a), again suggesting that a crossing from the S₂ to the S₁ is possible at the said geometry. The NH distances of the S₁ and the S₂ of compound 1 coincide at an OH length of 0.9 Å (Figure 4b), which represents a contraction from the equilibrating OH distance of any of the studied states (S₀, S₁, or S₂), and therefore would never be reached during an ESIPT reaction.

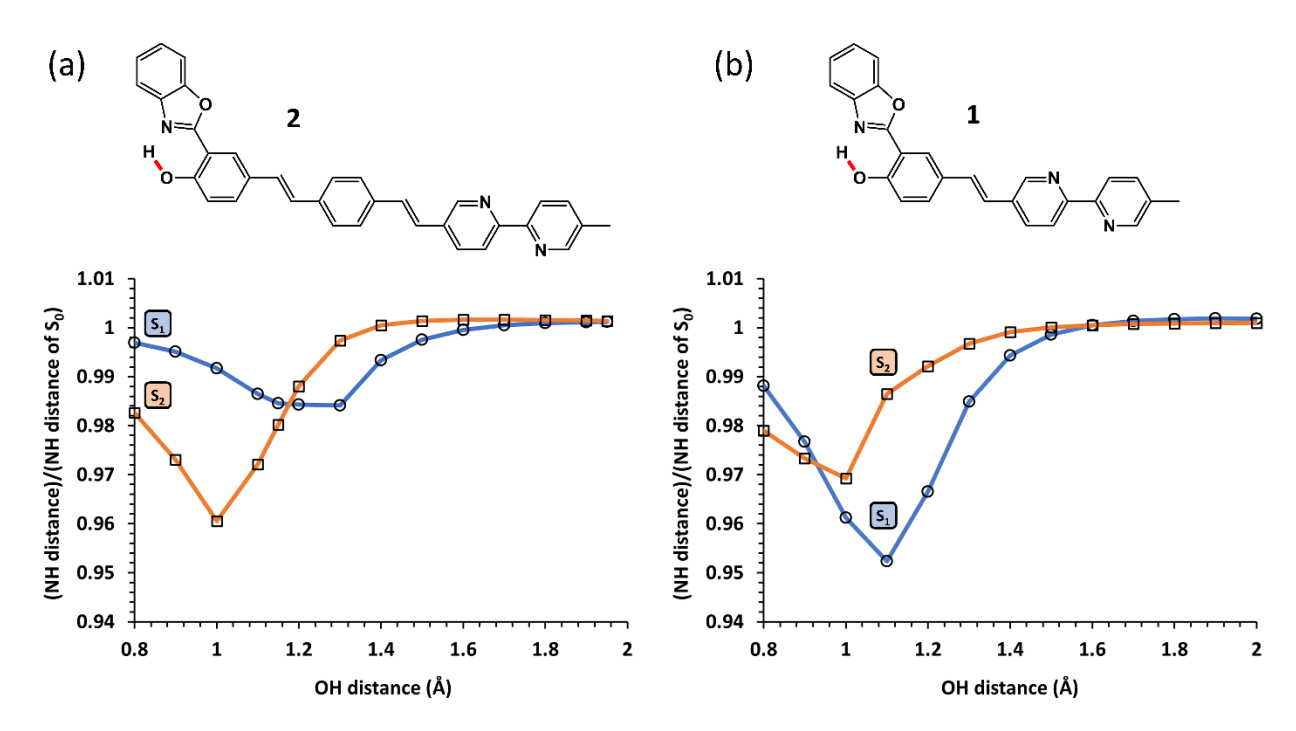


Figure 4. The ratios of the NH distances between the S_1 and the S_0 (blue) or the S_2 and the S_0 (orange) over the OH coordinates of compounds **2** (a), and **1** (b), calculated at the DFT or TDDFT/B3LYP/def2-TZVP level of theory. The structures of the compounds are shown above their MEPs. The OH bonds, the distances of which are the independent variables of the plots, are marked red in the structures.

Thirdly, the frontier molecular orbital (FMO) occupancies offer clues on the propensity of ESIPT on either the S₁ or the S₂. The displayed FMOs and data in Figure 5a,b were calculated using the RICC2/def2-TZVP method on the DFT/B3LYP/def2-TZVP-optimized ground state geometry. The results obtained using (TD)DFT/B3LYP/def2-TZVP method are shown in Figure S20, which led to the same conclusion. The S₁ state of 2 is primarily contributed by the transition from the HOMO to the LUMO. Both FMOs are localized on the stilbenoid component (Figure 5a). Therefore, the excitation to the S_1 has a high oscillator strength (2.96) and would not increase the basicity of the benzoxazole component as expected for the ESIPT. The excitation to the S₂ state, however, involves a charge transfer transition from the HOMO on the stilbenoid to the LUMO+1 on benzoxazole and has consequently a relatively small oscillator strength (0.22). Similar charge transfer transitions have been found in the excitations to the S₁ states of 5'substituted HBOs⁹ or the analogous HBTs (HBT= 2-(2-hydroxyphenyl)benzothiazole), ⁴⁹ which favor the ESIPT on the S₁ state. A more relevant example is the parent compound 1,8 the HOMO to LUMO (localized on stilbenoid) and HOMO to LUMO+1 (charge transfer to benzoxazole) transitions both contribute significantly to the S₁ and S₂ states (Figure 5b). Based on the oscillator strength values in comparison with those of compound 2 one may deduce that the S₁ state (a low oscillator strength of 0.26) shall lead to the ESIPT while the S₂ state (a high oscillator strength of 1.95) is principally localized on the stilbenoid. The very small gap between the S₁ and S₂ of compound 1 suggests that the internal conversion from S₂ to S₁ ought to be facile, and consequently the excitation to either excited state would trigger the ESIPT on the S₁. The comparison of the FMOs and the oscillator strength values of the S2 and S1 states between compounds 2 and 1 supports the conclusion that 2 undergoes ESIPT on the S₂ more efficiently than 1; the latter elects the S_1 as the surface for the ESIPT.

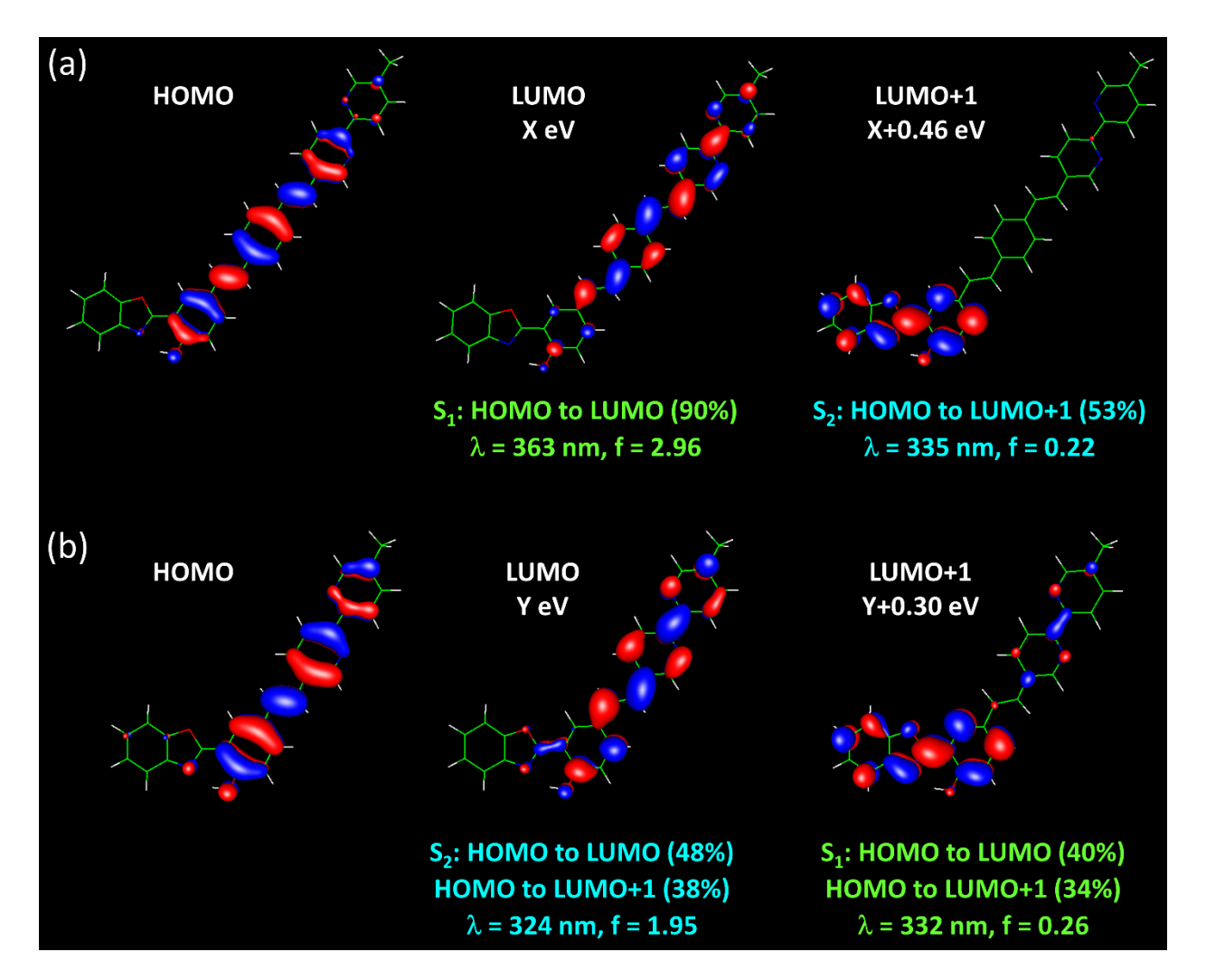


Figure 5. FMO diagrams of compounds **2** (a) and **1** (b) at the RICC2/def2-TZVP level of theory calculated on the DFT-optimized ground state geometries. The UMO energies are listed (relative to 'X' or 'Y'), so are the orbital contributions (%) and oscillator strengths (f) to the S₁ and S₂ states. The green and blue colors denote the S₁ and S₂ states, respectively.

Computational analysis yields the following factors that collectively lead to the excitation-dependent dual emission in an HBO derivative, without the assistance from the solvent or an additive (Figure 6). (1) The ESIPT on the S₁ state is endergonic so that the higher energy enol emission is a significant component of the total emission from the S₁ surface. Furthermore, for

the excitation dependence to emerge, there shall be no equilibrium of the ESIPT reaction on the S₁, based on the cogent arguments put forth by Chou and coworkers.⁵⁰ (2) On the S₂ surface, the FMO arrangement is such that it involves the HBO component, which triggers the ESIPT, and in a more physically intuitive description, the elongation of the OH bond and the contraction of the NH distance. (3) The ESIPT on the S₂ might complete adiabatically or via a crossing to the keto state on the S₁. Either way, the ESIPT initiated on the S₂ surface needs to be competitive with the internal conversion (IC) of the enol form to the S₁. The distinct electronic transitions of 2 to reach either the S₁ (restricted on the stilbenoid) or the S₂ (from stilbenoid to HBO) may create a barrier for the IC. Only when all three scenarios are materialized could excitation-dependent dual emission be observed. This model opens the door to future studies of verification, including more rigorous computational studies to distinguish the adiabatic and nonadiabatic ESIPT routes that start from the S₂ of the enol form, and the ultrafast absorption and emission spectroscopies for directly observing the competitions between IC and ESIPT in the excited states. Time resolved emission spectroscopy has been used to characterize the emission decays of an earlier example of ESIPT reaction on a higher electronically excited state. ⁵⁰ Time-resolved absorption spectroscopy has been carried out in a recent study of excitation-dependent electron transfer within an organic chromophore.⁵¹ ESIPT processes have been interrogated theoretically using different methods and conceptual frameworks, 40,52-54 which we intend to apply in the future to further describe the excited state chemistry of the current case from different angles. Quantitative benchmark values of the ESIPT reaction energy on the S₁ and the rates of ESIPT⁵⁵ and IC could also be provided from more comprehensive studies to aid the structural design of fluorophores capable of excitation-dependent dual emission.

S₂

N,

H-O

ESIPT (S₂)

$$(S_2 \text{ to } S_1)$$
 $(E_K - E_E)^{S_1} > 0$;

no equilibrium

 $(S_0 + S_1)$
 $(E_K - E_E)^{S_1} > 0$;

 $(E_K - E_E)^{S_1} > 0$;

Figure 6. A model of excitation-dependent dual emission of an HBO derivative.

Several processes may give rise to excitation-dependent dual (or multiple) emission. First, slow internal conversion (IC) from a higher excited state to the S₁ may render the emission from a higher excited state permissible as observed in azulene.⁵⁶ Such instances are rare,²⁸ which is consistent with the fact that most molecular fluorophores follow the Kasha's Rule.⁵⁷ Second, ground state equilibria between different forms of the dye, for example, conformational isomers, valence isomers,⁵⁸ solvent hydrogen-bonded⁸ or self-aggregated species, could lead to excitation-dependent multiple emission, if each ground state species is emissive and could be separately excited. Third, instead of emission from a higher electronically excited state, a chemical reaction might occur there that competes with the IC to the S₁. The choices of the reactions that are fast enough to compete with the IC, which usually occurs in the ps time scale, are quite limited. They primarily, if not exclusively, consist of proton transfer reactions, e.g., ESIPT.

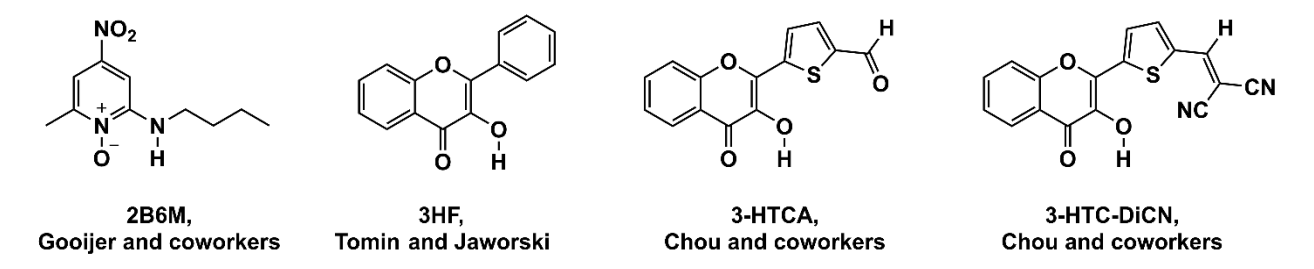


Figure 7. Four fluorescent compounds that were reported to undergo ESIPT from $S_n\ (n>1)$ states. 50,59

EXAMPLES of a small number of fluorescent compounds that have been reported to undergo ESIPT from an S_n (n > 1) state are shown in Figure 7. They include an alkylamino nitropyridine N-oxide⁵⁹ and substituted 3-hydroxyflavones.^{50,60} In these pioneering studies, features of dyes capable of excitation-dependent dual emission were postulated that overlap with the ones proposed in this study, which are specific to HBO derivatives. Due to the experimental and theoretical difficulties in studying excitation-dependent dual emission, later works have provided additions and modifications to the properties of these compounds and to the mechanistic models of these unusual ESIPT processes.⁶¹⁻⁶⁴ More cases of excitation-dependent ESIPT have continuously been reported,^{65,66} which are a reflection of the growing interests in developing emitters that respond to excitation energy. Comparing with these existing examples (Figure 7), compound 2 (1) is brighter (average fluorescence quantum yields $\phi_F = 0.18$ and 0.23 in DCM and toluene, respectively) with more balanced normal and tautomer emissions (close to white emission in both DCM and toluene, Figure 2), (2) has a closely related compound (1) to provide a contrast in the response to excitation energy, and (3) has a clear theoretical model to interpret the excitation-dependent dual emission.

Conclusion

In summary, contrasting to its parent compound 1, compound 2 exhibits excitation-dependent dual emission in solvents that preserve intramolecular hydrogen bonds. The excitation dependence has withstood rigorous control experiments, which have eliminated (1) ground state aggregation, (2) ground state conformational distribution, or (3) acid, base, or metal ion contamination as the cause of the excitation dependence. The consistent observations on this unique emission behavior from multiple independently prepared batches of compound 2 significantly reduces the likelihood that the excitation dependence could be attributed to inhomogeneity of the samples. All the experimental evidence supports the hypothesis that the provenance of the excitation dependence of dual emission from compound 2 is the ESIPT reaction on the S₂ state, rather than on the S₁ as ordinarily observed. This model is consistent with the computational analysis of the excited state behaviors of 2 against those of the similarly structured parent compound 1 that lacks the excitation dependence property. This work contributes to the fundamental molecular photophysics by uncovering a structural element that can be leveraged to control the normal vs tautomer emissions in ESIPT-capable fluorophores without the aid of external factors such as solvation, and the ratio of the two bands can be controlled by excitation energy. The derived photochemical model will be tested and refined in the future, and will be used to construct other molecules that are capable of excitation-dependent dual emission in non-polar environments.

ASSOCIATED CONTENT

Supporting Information. The following file is available free of charge at XXXXXX.

Synthetic procedures and characterization data, additional spectra and computation results (PDF)

AUTHOR INFORMATION

Corresponding author

Lei Zhu – Department of Chemistry and Biochemistry, Florida State University, 95 Chieftan Way, Tallahassee, FL 32306-4390, United States; orcid.org/0000-0001-8962-3666; Email lzhu@fsu.edu

Author

Joseph J. M. Hurley - Department of Chemistry and Biochemistry, Florida State University, 95 Chieftan Way, Tallahassee, FL 32306-4390, United States

Notes

The authors declare no competing financial interests.

ACKNOWLEDGMENT

This work was supported by the US National Science Foundation (CHE-1955262).

REFERENCES

- (1) Kwon, J. E.; Park, S. Y. Advanced Organic Optoelectronic Materials: Harnessing Excited-State Intramolecular Proton Transfer (ESIPT) Process. *Adv. Mater.* **2011**, *23*, 3615-3642.
- (2) Formosinho, S. J.; Arnaut, L. G. Excited-State Proton Transfer Reactions II. Intramolecular Reactions. *J. Photochem. Photobiol, A: Chem.* **1993**, *75*, 21-48.

- (3) Demchenko, A. P.; Tang, K.-C.; Chou, P.-T. Excited-State Proton Coupled Charge Transfer Modulated by Molecular Structure and Media Polarization. *Chem. Soc. Rev.* **2013**, *42*, 1379-1408.
- (4) Zhou, P.; Han, K. Unraveling the Detailed Mechanism of Excited-State Proton Transfer. *Acc. Chem. Res.* **2018**, *51*, 1681-1690.
- (5) Abou-Zied, O. K.; Jimenez, R.; Thompson, E. H. Z.; Millar, D. P.; Romesberg, F. E. Solvent-Dependent Photoinduced Tautomerization of 2-(2'-Hydroxyphenyl)benzoxazole. *J. Phys. Chem. A* **2002**, *106*, 3665-3672.
- (6) Yuan, Z.; Tang, Q.; Sreenath, K.; Simmons, J. T.; Younes, A. H.; Jiang, D.-e.; Zhu, L. Absorption and Emission Sensitivity of 2-(2'-Hydroxyphenyl)benzoxazole to Solvents and Impurities. *Photochem. Photobiol.* **2015**, *91*, 586-598.
- (7) Hurley, J. J. M.; Meisner, Q. J.; Guo, P.; Schaller, R. D.; Gosztola, D. J.; Wiederrecht, G. P.; Zhu, L. Triple Emission of 5'-(para-R-Phenylene)vinylene-2-(2'-hydroxyphenyl)benzoxazole (PVHBO). Part II: Emission from Anions. *J. Phys. Chem. A* **2022**, *126*, 1062-1075.
- (8) Meisner, Q. J.; Younes, A. H.; Yuan, Z.; Sreenath, K.; Hurley, J. J. M.; Zhu, L. Excitation-Dependent Multiple Fluorescence of a Substituted 2-(2'-Hydroxyphenyl)benzoxazole. *J. Phys. Chem. A* **2018**, *122*, 9209-9223.
- (9) Meisner, Q. J.; Hurley, J. J. M.; Guo, P.; Blood, A. R.; Schaller, R. D.; Gosztola, D. J.; Wiederrecht, G. P.; Zhu, L. Triple Emission of 5'-(para-R-Phenylene)vinylene-2-(2'-hydroxyphenyl)benzoxazole (PVHBO). Part I: Dual Emission from the Neutral Species. *J. Phys. Chem. A* **2022**, *126*, 1033-1061.
- (10) Seo, J.; Kim, S.; Park, S. Y. Strong Solvatochromic Fluorescence from the Intramolecular Charge-Transfer State Created by Excited-State Intramolecular Proton Transfer. *J. Am. Chem. Soc.* **2004**, *126*, 11154-11155.
- (11) Yang, Y.; Lowry, M.; Schowalter, C. M.; Fakayode, S. O.; Escobedo, J. O.; Xu, X.; Zhang, H.; Jensen, T. J.; Fronczek, F. R.; Warner, I. M.; Strongin, R. M. An Organic White Light-Emitting Fluorophore. *J. Am. Chem. Soc.* **2006**, *128*, 14081-14092.
- (12) D'Andrade, B. W.; Forrest, S. R. White Organic Light-Emitting Devices for Solid-State Lighting. *Adv. Mater.* **2004**, *16*, 1585-1595.
- (13) Benelhadj, K.; Muzuzu, W.; Massue, J.; Retailleau, P.; Charaf-Eddin, A.; Laurent, A. D.; Jacquemin, D.; Ulrich, G.; Ziessel, R. White Emitters by Tuning the Excited-State Intramolecular Proton-Transfer Fluorescence Emission in 2-(2'-Hydroxybenzofuran)benzoxazole Dyes. *Chem. Eur. J.* **2014**, *20*, 12843–12857.
- (14) Heyer, E.; Benelhadj, K.; Budzák, S.; Jacquemin, D.; Massue, J.; Ulrich, G. On the Fine-Tuning of the Excited-State Intramolecular Proton Transfer (ESIPT) Process in 2-(2'-Hydroxybenzofuran)benzazole (HBBX) Dyes. *Chem. Eur. J.* **2017**, *23*, 7324-7336.
- (15) Serdiuk, I. E. White Light from a Single Fluorophore: A Strategy Utilizing Excited-State Intramolecular Proton-Transfer Phenomenon and Its Verification. *J. Phys. Chem. C* **2017**, *121*, 5277-5286.
- (16) Zhang, Z.; Chen, Y.-A.; Hung, W.-Y.; Tang, W.-F.; Hsu, Y.-H.; Chen, C.-L.; Meng, F.-Y.; Chou, P.-T. Control of the Reversibility of Excited-State Intramolecular Proton Transfer (ESIPT) Reaction: Host-Polarity Tuning White Organic Light Emitting Diode on a New Thiazolo[5,4-d]thiazole ESIPT System. *Chem. Mater.* **2016**, *28*, 8815-8824.

- (17) Turro, N. J.; Ramamurthy, V.; Cherry, W.; Farneth, W. The effect of wavelength on organic photoreactions in solution. Reactions from upper excited states. *Chem. Rev.* **1978**, *78*, 125-145.
- (18) Demchenko, A. P.; Tomin, V. I.; Chou, P.-T. Breaking the Kasha Rule for More Efficient Photochemistry. *Chem. Rev.* **2017**, *117*, 13353-13381.
- (19) Malpicci, D.; Lucenti, E.; Giannini, C.; Forni, A.; Botta, C.; Cariati, E. Prompt and Long-Lived Anti-Kasha Emission from Organic Dyes. *Molecules* **2021**, *26*, 6999.
- (20) Ahlrichs, R.; Bär, M.; Häser, M.; Horn, H.; Kölmel, C. Electronic Structure Calculations on Workstation Computers: The Program System Turbomole. *Chem. Phys. Lett.* **1989**, *162*, 165-169.
- (21) Lee, C.; Yang, W.; Parr, R. G. Development of the Colle-Salvetti Correlation-Energy Formula into a Functional of the Electron Density. *Phys. Rev. B* **1988**, *37*, 785-789.
- (22) Weigend, F.; Ahlrichs, R. Balanced Basis Sets of Split Valence, Triple Zeta Valence and Quadruple Zeta Valence Quality for H to Rn: Design and Assessment of Accuracy. *Phys. Chem. Phys.* **2005**, *7*, 3297-3305.
- (23) Adamo, C.; Jacquemin, D. The Calculations of Excited-State Properties with Time-Dependent Density Functional Theory. *Chem. Soc. Rev.* **2013**, *42*, 845-856.
- (24) Laaksonen, L. A Graphics Program for the Analysis and Display of Molecular Dynamics Trajectories. *J. Mol. Graph.* **1992**, *10*, 33-34.
- (25) Bergman, D. L.; Laaksonen, L.; Laaksonen, A. Visualization of Solvation Structures in Liquid Mixtures. *J. Mol. Graph.* **1997**, *15*, 301-306.
- (26) Raoui, M.; Massue, J.; Azarias, C.; Jacquemin, D.; Ulrich, G. Highly Fluorescent Extended 2-(2'-hydroxyphenyl)benzazole Dyes: Synthesis, Optical Properties and First-Principle Calculations. *Chem. Commun.* **2016**, *52*, 9216-9219.
- (27) Shafikov, M. Z.; Brandl, F.; Dick, B.; Czerwieniec, R. Can Coumarins Break Kasha's Rule? *J. Phys. Chem. Lett.* **2019**, *10*, 6468-6471.
- (28) del Valle, J. C.; Catalán, J. Kasha's rule: a reappraisal. *Phys. Chem. Chem. Phys.* **2019**, *21*, 10061-10069.
- (29) Tirado-Rives, J.; Jorgensen, W. L. Performance of B3LYP Density Functional Methods for a Large Set of Organic Molecules. *J. Chem. Theory Comput.* **2008**, *4*, 297-306.
- (30) Teramae, H.; Nagaoka, S.-i.; Nagashima, U. COMPUTATIONAL STUDY OF EXCITED-STATE INTRAMOLECULAR-PROTON-TRANSFER OF O-HYDROXYBENZALDEHYDE, O-FORMYL-SUBSTITUTED PHENOLS, AND 5-SUBSTITUTED SALICYLALDEHYDES *Int. J. Chem. Model.* **2012**, *4*, 269-287.
- (31) de Vivie-Riedle, R.; De Waele, V.; Kurtz, L.; Riedle, E. Ultrafast Excited-State Proton Transfer of 2-(2'-Hydroxyphenyl)benzothiazole: Theoretical Analysis of the Skeletal Deformations and the Active Vibrational Modes. *J. Phys. Chem. A* **2003**, *107*, 10591-10599.
- (32) Aquino, A. J. A.; Lischka, H.; Hättig, C. Excited-State Intramolecular Proton Transfer: A Survey of TDDFT and RI-CC2 Excited-State Potential Energy Surfaces. *J. Phys. Chem. A* **2005**, *109*, 3201-3208.
- (33) Georgieva, I.; Trendafilova, N.; Aquino, A. J. A.; Lischka, H. Excited-State Proton Transfer in 7-Hydroxy-4-methylcoumarin along a Hydrogen-Bonded Water Wire. *J. Phys. Chem. A* **2007**, *111*, 127-135.
- (34) García, R.; More, S.; Melle-Franco, M.; Mateo-Alonso, A. 11,11,12,12-Tetracyano-4,5-pyrenoquinodimethanes: Air-Stable Push–Pull o-Quinodimethanes with S2 Fluorescence. *Org. Lett.* **2014**, *16*, 6096-6099.

- (35) Liu, Z.-Y.; Hu, J.-W.; Huang, C.-H.; Huang, T.-H.; Chen, D.-G.; Ho, S.-Y.; Chen, K.-Y.; Li, E. Y.; Chou, P.-T. Sulfur-Based Intramolecular Hydrogen-Bond: Excited-State Hydrogen-Bond On/Off Switch with Dual Room-Temperature Phosphorescence. *J. Am. Chem. Soc.* **2019**, *141*, 9885-9894.
- (36) Feng, C.; Li, S.; Fu, L.; Xiao, X.; Xu, Z.; Liao, Q.; Wu, Y.; Yao, J.; Fu, H. Breaking Kasha's Rule as a Mechanism for Solution-Phase Room-Temperature Phosphorescence from High-Lying Triplet Excited State. *J. Phys. Chem. Lett.* **2020**, *11*, 8246-8251.
- (37) Jhun, B. H.; Jeong, D. Y.; Nah, S.; Park, S. Y.; You, Y. Novel anti-Kasha fluorophores exhibiting dual emission with thermally activated delayed fluorescence through detouring triplet manifolds. *J. Mater. Chem. C* **2021**, *9*, 7083-7093.
- (38) Sobolewski, A. L.; Domcke, W. Photophysics of Malonaldehyde: An ab Initio Study. *J. Phys. Chem. A* **1999**, *103*, 4494-4504.
- (39) L. Sobolewski, A.; Domcke, W. Abinitio Potential-Energy Functions for Excited State Intramolecular Proton Transfer: a Comparative Study of o-Hydroxybenzaldehyde, Salicylic Acid and 7-Hydroxy-1-indanone. *Phys. Chem. Chem. Phys.* **1999**, *1*, 3065-3072.
- (40) Sobolewski, A. L.; Domcke, W. Computational Studies of the Photophysics of Hydrogen-Bonded Molecular Systems. *J. Phys. Chem. A* **2007**, *111*, 11725-11735.
- (41) Yin, H.; Li, H.; Xia, G.; Ruan, C.; Shi, Y.; Wang, H.; Jin, M.; Ding, D. A Novel Non-Fluorescent Excited State Intramolecular Proton Transfer Phenomenon Induced by Intramolecular Hydrogen Bonds: an Experimental and Theoretical Investigation. *Sci. Rep.* **2016**, *6*, 19774.
- (42) Raeker, T.; Hartke, B. Full-Dimensional Excited-State Intramolecular Proton Transfer Dynamics of Salicylic Acid. *J. Phys. Chem. A* **2017**, *121*, 5967-5977.
- (43) Chudoba, C.; Riedle, E.; Pfeiffer, M.; Elsaesser, T. Vibrational coherence in ultrafast excited state proton transfer. *Chem. Phys. Lett.* **1996**, *263*, 622-628.
- (44) Stock, K.; Bizjak, T.; Lochbrunner, S. Proton transfer and internal conversion of o-hydroxybenzaldehyde: coherent versus statistical excited-state dynamics. *Chem. Phys. Lett.* **2002**, *354*, 409-416.
- (45) Lochbrunner, S.; Wurzer, A. J.; Riedle, E. Microscopic Mechanism of Ultrafast Excited-State Intramolecular Proton Transfer: A 30-fs Study of 2-(2°-Hydroxyphenyl)benzothiazole. *J. Phys. Chem. A* **2003**, *107*, 10580-10590.
- (46) Takeuchi, S.; Tahara, T. Coherent Nuclear Wavepacket Motions in Ultrafast Excited-State Intramolecular Proton Transfer: Sub-30-fs Resolved Pump-Probe Absorption Spectroscopy of 10-Hydroxybenzo[h]quinoline in Solution. *J. Phys. Chem. A* **2005**, *109*, 10199-10207.
- (47) Schriever, C.; Barbatti, M.; Stock, K.; Aquino, A. J. A.; Tunega, D.; Lochbrunner, S.; Riedle, E.; de Vivie-Riedle, R.; Lischka, H. The interplay of skeletal deformations and ultrafast excited-state intramolecular proton transfer: Experimental and theoretical investigation of 10-hydroxybenzo[h]quinoline. *Chem. Phys.* **2008**, *347*, 446-461.
- (48) Schriever, C.; Lochbrunner, S.; Ofial, A. R.; Riedle, E. The origin of ultrafast proton transfer: Multidimensional wave packet motion vs. tunneling. *Chem. Phys. Lett.* **2011**, *503*, 61-65.
- (49) Xu, L.; Wang, Q.; Zhang, Y. Electronic effect on the photophysical properties of 2-(2-hydroxyphenyl)benzothiazole-based excited state intramolecular proton transfer fluorophores synthesized by Sonogashira-coupling reaction. *Dyes Pigm.* **2017**, *136*, 732-741.

- (50) Tseng, H.-W.; Shen, J.-Y.; Kuo, T.-Y.; Tu, T.-S.; Chen, Y.-A.; Demchenko, A. P.; Chou, P.-T. Excited-state intramolecular proton-transfer reaction demonstrating anti-Kasha behavior. *Chem. Sci.* **2016**, *7*, 655-665.
- (51) Jones, A. L.; Jiang, J.; Schanze, K. S. Excitation-Wavelength-Dependent Photoinduced Electron Transfer in a π-Conjugated Diblock Oligomer. *J. Am. Chem. Soc.* **2020**, *142*, 12658-12668.
- (52) Houari, Y.; Charaf-Eddin, A.; Laurent, A. D.; Massue, J.; Ziessel, R.; Ulrich, G.; Jacquemin, D. Modeling Optical Signatures and Excited-State Reactivities of Substituted Hydroxyphenylbenzoxazole (HBO) ESIPT Dyes. *Phys. Chem. Chem. Phys.* **2014**, *16*, 1319-1321.
- (53) Wu, C.-H.; Karas, L. J.; Ottosson, H.; Wu, J. I.-C. Excited-state proton transfer relieves antiaromaticity in molecules. *Proc. Nat. Acad. Sci.* **2019**, *116*, 20303-20308.
- (54) Lampkin, B. J.; Nguyen, Y. H.; Karadakov, P. B.; VanVeller, B. Demonstration of Baird's rule complementarity in the singlet state with implications for excited-state intramolecular proton transfer. *Phys. Chem. Chem. Phys.* **2019**, *21*, 11608-11614.
- (55) Kim, C. H.; Park, J.; Seo, J.; Park, S. Y.; Joo, T. Excited State Intramolecular Proton Transfer and Charge Transfer Dynamics of a 2-(2'-Hydroxyphenyl)benzoxazole Derivative in Solution. *J. Phys. Chem. A* **2010**, *114*, 5618-5629.
- (56) Beer, M.; Longuet-Higgins, H. C. Anomalous Light Emission of Azulene. *J. Chem. Phys.* **1955**, *23*, 1390-1391.
- (57) Kasha, M. Characterization of Electronic Transitions in Complex Molecules. *Discuss. Faraday Soc.* **1950**, *6*, 14-19.
- (58) Craig, I. M.; Duong, H. M.; Wudl, F.; Schwartz, B. J. A New Route to Dual Fluorescence: Spectroscopic Properties of the Valence Tautomers of a 3-(2H)-Isoquinolinone Derivative. *Chem. Phys. Lett.* **2009**, *477*, 319-324.
- (59) de Klerk, J. S.; Szemik-Hojniak, A.; Ariese, F.; Gooijer, C. Intramolecular Proton-Transfer Processes Starting at Higher Excited States: A Fluorescence Study on 2-Butylamino-6-methyl-4-nitropyridine N-Oxide in Nonpolar Solutions. *J. Phys. Chem. A* **2007**, *111*, 5828-5832.
- (60) Tomin, V. I.; Jaworski, R. ESIPT reaction starting from S2 and S3 singlet states in 3-hydroxyflavone. *Eur. Phys. J. Spec. Top.* **2007**, *144*, 123-128.
- (61) Klerk, J. d.; van Stokkum, I. H. M.; Szemik-Hojniak, A.; Deperasińska, I.; Gooijer, C.; Zhang, H.; Buma, W.-J.; Ariese, F. Excited State Processes of 2-Butylamino-6-methyl-4-nitropyridine N-oxide in Nonpolar Solvents. A Transient Absorption Spectroscopy Study. *J. Phys. Chem. A* **2010**, *114*, 4045-4050.
- (62) Yuan, H.; Guo, X.; Zhang, J. Ab initio insights into the mechanism of excited-state intramolecular proton transfer triggered by the second excited singlet state of a fluorescent dye: an anti-Kasha behavior. *Mater. Chem. Front.* **2019**, *3*, 1225-1230.
- (63) Makarewicz, A.; Szemik-Hojniak, A.; van der Zwan, G.; Deperasińska, I. Excited-State Forms of 2-Methylamino-6-methyl-4-nitropyridine N-Oxide and 2-Butylamino-6-methyl-4-nitropyridine N-Oxide. *J. Phys. Chem. A* **2009**, *113*, 3438-3446.
- (64) Huang, J.-D.; Zhang, J.; Chen, D.; Ma, H. Density functional theoretical investigation of intramolecular proton transfer mechanisms in the derivatives of 3-hydroxychromone. *Org. Chem. Front.* **2017**, *4*, 1812-1818.

- (65) Georgiev, A.; Yordanov, D.; Vassilev, N.; Deneva, V.; Nedeltcheva, D.; Angelov, I.; Antonov, L. A single isomer rotary switch demonstrating anti-Kasha behaviour: Does acidity function matter? *Phys. Chem. Chem. Phys.* **2021**, *23*, 13760-13767.
- (66) Shekhovtsov, N. A.; Nikolaenkova, E. B.; Berezin, A. S.; Plyusnin, V. F.; Vinogradova, K. A.; Naumov, D. Y.; Pervukhina, N. V.; Tikhonov, A. Y.; Bushuev, M. B. A 1-Hydroxy-1H-imidazole ESIPT Emitter Demonstrating anti-Kasha Fluorescence and Direct Excitation of a Tautomeric Form. *ChemPlusChem* **2021**, *86*, 1436-1441.